Resonance Raman microprobe spectroscopy of rhodopsin mutants: Effect of substitutions in the third transmembrane helix

ARTICLE *in* BIOCHEMISTRY · JULY 1992

Impact Factor: 3.02 · DOI: 10.1021/bi00137a003 · Source: PubMed

5 AUTHORS, INCLUDING:

Thomas Sakmar
The Rockefeller University
218 PUBLICATIONS **10,841** CITATIONS

SEE PROFILE

Articles

Resonance Raman Microprobe Spectroscopy of Rhodopsin Mutants: Effect of Substitutions in the Third Transmembrane Helix†

Steven W. Lin,‡ Thomas P. Sakmar,§,∥ Roland R. Franke,∥,⊥ H. Gobind Khorana,∥ and Richard A. Mathies*,‡

Department of Chemistry, University of California, Berkeley, California 94720, Howard Hughes Medical Institute, Rockefeller University, New York, New York 10021, and Departments of Biology and Chemistry, Massachusetts Institute of Technology, Cambridge, Massachusetts 60639

Received December 23, 1991; Revised Manuscript Received March 19, 1992

ABSTRACT: A microprobe system has been developed that can record Raman spectra from as little as 2 μL of solution containing only micrograms of biological pigments. The apparatus consists of a liquid nitrogen (l-N_2)-cooled cold stage, an epi-illumination microscope, and a subtractive-dispersion, double spectrograph coupled to a l-N_2-cooled CCD detector. Experiments were performed on native bovine rhodopsin, rhodopsin expressed in COS cells, and four rhodopsin mutants: Glu^{134} replaced by Gln (E134Q), Glu^{122} replaced by Gln (E122Q), and Glu^{113} replaced by Gln (E113Q) or Ala (E113A). Resonance Raman spectra of photostationary steady-state mixtures of 11-*cis*-rhodopsin, 9-*cis*-isorhodopsin, and *all-trans*-bathorhodopsin at 77 K were recorded. The Raman spectra of E134Q and the wild-type are the same, indicating that Glu^{134} is not located near the chromophore. Substitution at Glu^{122} also does not affect the C=NH stretching vibration of the chromophore. The fingerprint and Schiff base regions of the Raman spectra of the 380-nm, pH 7 forms of E113Q and E113A are characteristic of unprotonated retinal Schiff bases. The C=NH modes of the ~500-nm, pH 5 forms of E113Q and E113A in H_2O (D_2O) are found at 1648 (1629) and 1645 (1630) cm^{-1}, respectively. These frequencies indicate that the protonated Schiff base interacts more weakly with its protein counterion in the Glu^{113} mutants than it does in the native pigment. Furthermore, perturbations of the unique bathorhodopsin hydrogen out-of-plane (HOOP) vibrations in E113Q and E113A indicate that the strength of the protein perturbation near C_{12} is weakened compared to that in native bathorhodopsin. These results are consistent with a picture in which the carboxylate group of Glu^{113} stabilizes the protonated Schiff base and also perturbs the C_{12}-position of the chromophore.

Rhodopsin, the visual pigment of the retinal rod cell, consists of a seven-helix integral membrane protein and an 11-*cis*-retinal chromophore bound to Lys^{296} via a protonated Schiff base linkage. The absorption maxima (λ_{max}) of rhodopsin and its photointermediates are determined by unique interactions between the chromophore and the amino acid residues in the chromophore binding site. A variety of biophysical techniques have been used to examine the molecular basis of these chromophore–protein interactions [for reviews, see Birge (1990) and Ottolenghi and Sheves (1989)]. However, the mechanism of λ_{max} regulation is not yet understood.

The structure and environment of the retinal chromophore in bovine rhodopsin and its photointermediates have been investigated extensively using resonance Raman spectroscopy (Deng & Callender, 1987; Doukas et al., 1978; Eyring & Mathies, 1979; Mathies et al., 1987; Palings et al., 1987, 1989) and solid-state NMR (Smith et al., 1990, 1991). The results of these studies are consistent with the existence of a negative counterion that is hydrogen-bonded to the positively charged protonated Schiff base (PSB)[1] (Blatz et al., 1972; Honig et al., 1976) and a perturbation near the C_{12}-position of the polyene chain. Site-specific mutagenesis (Nathans, 1990a; Sakmar et al., 1989; Zhukovsky & Oprian, 1989) has provided strong evidence against the suggestion that there is a second negatively charged residue in the binding pocket that perturbs the chromophore near the C_{11}=C_{12} bond (Honig et al., 1979; Koutalos et al., 1989). This conclusion is consistent with the results and analysis of two-photon absorption experiments (Birge et al., 1985).

The Schiff base counterion in bovine rhodopsin is now known to be Glu^{113} (Nathans, 1990b; Sakmar et al., 1989; Zhukovsky & Oprian, 1989). Replacement of Glu^{113} by a neutral amino acid lowers the Schiff base pK_a to ~6, and the protein forms a pH-dependent mixture of ~500-nm-absorbing (acidic) and 380-nm-absorbing (basic) species. It was proposed that the 380-nm absorbance in the basic pigment is due to an unprotonated retinal Schiff base chromophore (Sakmar et al., 1989; Zhukovsky & Oprian, 1989). A mutagenesis-based model for the protein environment around the chromophore in rhodopsin has been presented (Nakayama & Khorana, 1991). However, the secondary interactions between the protein and the chromophore that are responsible for its unique

† This research was supported by the National Institutes of Health (EY 02051 to R.A.M., GM 28289 and AI 11479 to H.G.K.), the Office of Naval Research (N00014-82-K-0189 to H.G.K.), and the Howard Hughes Medical Institute (to T.P.S.).

* Address correspondence to this author.
‡ University of California.
§ Howard Hughes Medical Institute, Rockefeller University.
∥ Massachusetts Institute of Technology.
⊥ Present address: Howard Hughes Medical Institute, Rockefeller University, New York, NY 10021.

[1] Abbreviations: CCD, charge-coupled device; HOOP, hydrogen out-of-plane; PSB, protonated Schiff base of retinal; ROS, rod outer segment; rhodopsin mutants are designated by the wild-type amino acid residue (single-letter code) and its position number followed by the substituted amino acid residue.

0006-2960/92/0431-5105$03.00/0

properties have not been determined.

To understand chromophore structure and function in rhodopsin, atomic-resolution information about the binding site is needed. Resonance Raman vibrational spectroscopy on site-specific mutants can provide this detailed structural information. However, it has not been feasible to carry out resonance Raman experiments on rhodopsin mutants because of the low abundance (<0.1 mg) of these photolabile proteins. We therefore became interested in using the resonance Raman microprobe (Rosasco, 1980) to study rhodopsin mutants. This technique has enabled Raman studies of lymph nodes (Abraham & Etz, 1979), visual pigments in single vertebrate photoreceptor cells (Barry & Mathies, 1982, 1987; Barry et al., 1987; Loppnow et al., 1989), protein microcrystals (Smulevich et al., 1990), and single cells and their chromosomes (Puppels et al., 1990), but it has not been used to study small quantities of expressed proteins.

We demonstrate here that resonance Raman microprobe spectra can be obtained from as little as ~8 μg of pigment using a recently developed liquid nitrogen (l-N_2) cold stage (Loppnow & Mathies, 1989) and by exploiting the sensitivity of a l-N_2-cooled CCD detector. Raman microprobe experiments were performed on purified, detergent-solubilized samples of recombinant rhodopsin and a set of site-directed mutants (E134Q, E122Q, E113Q, and E113A) altered on the third transmembrane helix. These vibrational spectra provide structural evidence for a direct electrostatic interaction of the retinal Schiff base with its Glu^{113} counterion. Furthermore, the effect of Glu^{113} substitution on the low-wavenumber lines of bathorhodopsin, the primary photoproduct, shed light on the nature of the chromophore–Glu^{113} interaction. These data are used to develop a refined molecular model of the chromophore binding site in rhodopsin.

Materials and Methods

Preparation of Rhodopsin Mutants. Mutagenesis of the synthetic opsin gene (Ferretti et al., 1986) to produce the E113Q, E113A, E122Q, and E134Q mutants was previously reported (Sakmar et al., 1989, 1991). COS-1 cells were transiently transfected with opsin genes, harvested, and regenerated with 11-*cis*-retinal (Franke et al., 1988; Oprian et al., 1987). About 75–125 tissue culture plates (100 mm) of COS cells were transfected for each set of experiments. Purification of the mutant pigments was carried out by an immunoaffinity adsorption procedure (Oprian et al., 1987) except that cells were solubilized in 1% dodecyl maltoside buffer and washes were carried out in 25 mM Tris-HCl, pH 6.8, 50 mM NaCl, and 0.05% dodecyl maltoside (Sakmar et al., 1989). E113Q and E113A were prepared in 50 mM NaCl and 0.1% dodecyl maltoside in H_2O or D_2O by washing the immunoaffinity resin extensively with the appropriate solution and eluting from the resin into the same solution. Pigments were eluted 2 or 3 times with final elution volumes of 7.5 mL. Samples were concentrated to about 100 μL by filtration using Centricon-30 filters (Amicon) and in some cases by subsequent evaporation in a desiccator jar over calcium sulfate. Native rhodopsin was purified from solubilized ROS by the same procedure. UV–visible absorbance spectroscopy was performed on each concentrated pigment sample. Yields ranged from 70 to 100 μL with 0.9–2.4 absorbance units/cm at the visible λ_{max} of the pigment.

Raman Spectroscopy. Resonance Raman spectra of the pigments were obtained using the Raman microprobe apparatus illustrated in Figure 1. A detailed description of the cold stage and the procedures for sample introduction and cooling have been published (Loppnow & Mathies, 1989). To

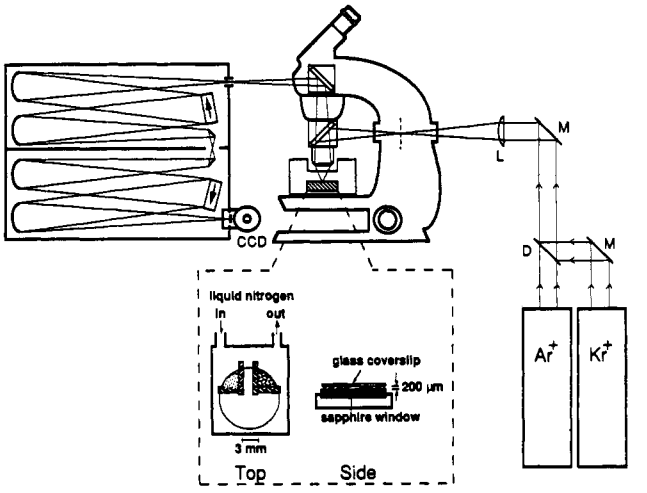

FIGURE 1: Raman microprobe system. Laser light from the Ar^+ and Kr^+ lasers is focused on the sample by a 40× long-working-length objective lens. Back-scattered light collected by the objective lens is coupled into the spectrograph, dispersed, and focused onto the l-N_2-cooled unintensified CCD detector. The pigment and its bleached blank are frozen on separate quadrants of the cold-stage sapphire window at 77 K. M, mirror; D, dichroic beam splitter; L, cylindrical lens.

define the location and the path length of the sample, two cells are made on the sapphire window by placing thin strips of double-sided tape (TEMP-R-TAPE M-69, CHR Industries) on the substrate with the pattern shown in Figure 1. A glass coverslip (0.2-mm thickness) is then placed over the tape. The cell dimension is ~3 mm × 2 mm × 200 μm. About 2 μL of pigment solution is applied into one cell using a syringe, and the same amount of bleached pigment is applied to the adjacent cell. The temperature of the cell is lowered to 77 K by flowing liquid N_2 through the cold tip, and the cold-stage is evacuated to prevent condensation. The frozen sample forms an opaque glass.

Raman excitation in the visible was performed using a 488.0-nm probe beam (~5 mW at sample, Spectra-Physics 2020-05 Ar^+ laser) and a coaxial 568.2-nm pump beam (~7 mW at sample, Spectra-Physics 2025-11 Kr^+ laser). The 380-nm pigment of E113Q was probed with 413.1-nm light (~5 mW at sample). The beams were first focused with a 250-mm cylindrical lens at the microscope focal plane. The line image of the beam was then focused on the sample by the 40× NA 0.6 objective lens (corrected for a 1-mm cover slip) to form a ~5 × 100 μm illuminated area. Back-scattered Raman light was collected by the same high-NA objective and focused at the entrance slit of the subtractive-dispersion, double spectrograph (Mathies & Yu, 1978). Stray probe light was minimized by placing a long-pass filter (Schott GG-495 and GG-420 for 488- and 413.1-nm excitation, respectively) at the entrance slit. Stray light from the 568.2 pump was rejected by a short-pass filter (Ditric Optics, 50% cutoff at 540 nm).

Raman scattering was detected with a cryogenically cooled CCD detector (LN/CCD-1152, Princeton Instruments) controlled by an ST-130 controller (Princeton Instruments). The CCD detector contains a 1152 × 298 pixel array with a 26 × 6.7 mm photosensitive area that is read out with a 16-bit A/D converter. The advantages of this detector are high dynamic range, high quantum sensitivity (~50% at 730 nm), negligible dark noise (1 count h^{-1} $pixel^{-1}$), low detector read-out noise (1 count/read), and broad spectral coverage (~1400 cm^{-1} in the visible).

In these experiments, the Raman scattering was collected from a ~5 × 100 μm area approximately 50 μm below the

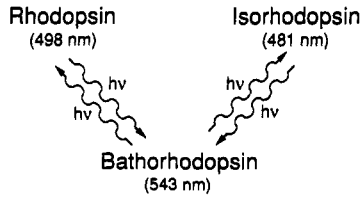

FIGURE 2: Rhodopsin, isorhodopsin, and bathorhodopsin form a photostationary steady-state mixture when irradiated at 77 K. The absorption maxima of the pigments are indicated in parentheses. The geometry of the PSB chromophore is 11-cis in rhodopsin, 9-cis in isorhodopsin, and all-trans in bathorhodopsin.

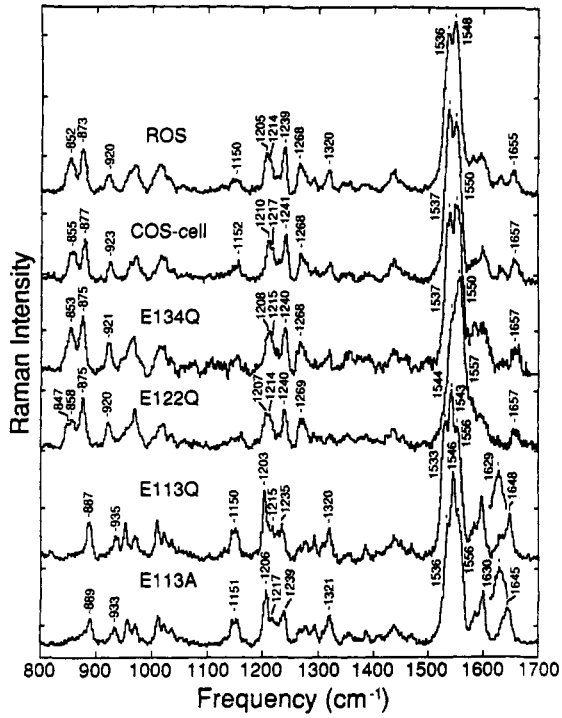

FIGURE 3: Raman microprobe spectra of native rhodopsin from rod outer segments (ROS), wild-type rhodopsin expressed in COS cells, and the site-directed mutants E134Q, E122Q, E113Q, and E113A in H_2O. The E113Q and E113A spectra were obtained at pH ~5. For E113Q and E113A, the Schiff base regions of spectra recorded in a D_2O buffer are also shown. Each spectrum was obtained using 488.0-nm excitation from ~5 μL of pigment solution frozen at 77 K. The Raman spectra of ROS rhodopsin, E134Q, and E122Q were recorded with a dry-ice-cooled vidicon detector. It was necessary to record two overlapping windows with this system to cover the spectral region. Because of the reduced sensitivity of this earlier system, about 10 μL of ROS, E134Q, and E122Q pigments was required.

surface of the frozen sample. Collection from this depth minimized stray reflected light and gave more reproducible background subtractions. It was typically necessary to record 10 ~3-min exposures from the pigment and bleached-pigment regions to obtain spectra of sufficient signal-to-noise. A single 3-min exposure contained about 2000 Raman counts in the ethylenic line on top of a ~40 000-count fluorescence background. Each exposure was recorded from a new sample area. Approximately 5 μL of pigment with an absorbance of ~1.5 OD/cm at the λ_{max} was used in each round of experiments. The fluorescence background was removed by subtracting a bleached-pigment spectrum. Frequencies were assigned using atomic transition lines from a hollow iron cathode lamp. The reported frequencies are accurate to within 2 cm^{-1}, and the resolution of the spectra is 6 cm^{-1}.

RESULTS

The wild-type COS cell rhodopsin and the mutant pigments E134Q, E122Q, E113Q, and E113A were characterized

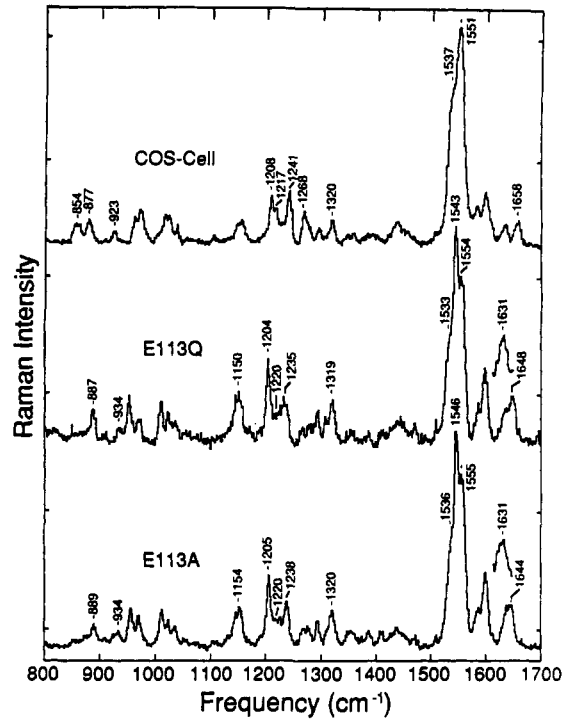

FIGURE 4: Pump–probe Raman microprobe spectra of wild-type rhodopsin expressed in COS cells and in E113Q and E113A mutants in H_2O at 77 K. The E113Q and E113A spectra were obtained at pH ~5. The Schiff base regions for E113Q and E113A in D_2O are also shown. These spectra were obtained using a 488.0-nm probe and 568.2-nm pump with a pump:probe power ratio of 1.3:1.

previously by biochemical assays and UV–visible spectroscopy (Sakmar et al., 1989, 1991). After preparation and concentration, ROS rhodopsin, COS cell rhodopsin, and E134Q displayed λ_{max} values of 498 nm while the λ_{max} of E122Q was 481 nm. Both E113Q and E113A existed as pH-dependent equilibrium mixtures of visible-absorbing (acidic) and near-UV-absorbing (basic) forms. The λ_{max} values for the visible forms of E113Q and E113A at pH ~5 in H_2O (D_2O) were 492 (499) and 505 (507) nm, respectively. The λ_{max} values of the basic forms of E113Q and E113A at pH ~7 were both ~380 nm. The protein concentration procedure did not lead to significant denaturation or changes in UV–visible spectral characteristics.

Resonance Raman microprobe spectra were obtained from a photostationary steady-state mixture of rhodopsin, isorhodopsin, and bathorhodopsin at 77 K [see Figure 2 and Yoshizawa and Wald (1963)]. The relative composition of rhodopsin, bathorhodopsin, and isorhodopsin can be varied by using a different probe wavelength or by adding pump illumination (Eyring & Mathies, 1979; Oseroff & Callender, 1974). For example, a coaxial yellow or red pump preferentially depletes the redder-absorbing bathorhodopsin population. Using this technique, vibrational lines which decrease in intensity in the presence of the yellow 568.2-nm pump can be assigned to bathorhodopsin.

The 488-nm probe-only resonance Raman spectra of ROS and COS cell rhodopsins and the three mutants are displayed in Figure 3. Comparison of the Raman spectrum of COS cell rhodopsin with that of native ROS rhodopsin indicates that no significant perturbations are introduced by the COS cell preparation. The three bands at 855, 877, and 923 cm^{-1}, which decrease in intensity in the pump–probe spectrum (Figure 4), are assigned to the hydrogen out-of-plane (HOOP) vibrations of bathorhodopsin in the COS cell sample. The frequencies and the relative intensities of the HOOP, fin-

gerprint, and ethylenic modes are similar to those of the ROS sample. There is a small ~2 cm^{-1} shift of the C=NH stretching and fingerprint vibrations in COS cell rhodopsin which may indicate small differences in the binding pocket environment.

The substitution of Gln for Glu^{134} has a minimal effect on the Raman spectrum. The relative intensities and the frequencies of the modes, in particular the C=NH stretch, are identical to those of COS cell rhodopsin. Previous biochemical studies of E134Q showed that this mutant has a normal λ_{max} (Nathans, 1990a; Sakmar et al., 1989) and the ability to activate transducin (Sakmar et al., 1989). The resonance Raman spectra of E134Q are consistent with these earlier observations.

Larger perturbations of chromophore structure are seen in the E122Q mutant. The 1657-cm^{-1} Schiff base stretching mode is at the same frequency as in the wild-type, and the fingerprint lines also appear normal. However, the ethylenic bands assigned to isorhodopsin and bathorhodopsin are upshifted ~7 cm^{-1} to 1557 and 1544 cm^{-1}, respectively. On the basis of the inverse linear relationship between the λ_{max} value and the C=C stretching frequency of retinal polyenes (Doukas et al., 1978; Rimai et al., 1973), the upshifted ethylenics reflect blue-shifts of the bathorhodopsin and isorhodopsin absorption maxima to approximately 515 and 460 nm, respectively. The different relative intensities of the ethylenic peaks in the spectrum are due to the change in the extinction coefficients of rhodopsin, isorhodopsin, and bathorhodopsin at the Raman probe wavelength in the E122Q mutant which results from the ~20-nm blue-shifts of their absorption bands compared to the wild-type protein.

The HOOP vibrations of bathorhodopsin are also affected by the substitution at Glu^{122}. In native bathorhodopsin, the HOOP region consists of four modes: C_{14}–H wag at 850 cm^{-1}, C_{12}–H wag at 858 cm^{-1}, C_{10}–H wag combination at 875 cm^{-1}, and C_{11}–H wag at 921 cm^{-1} (Palings et al., 1989). These vibrations are clearly visible in the COS cell rhodopsin, E134Q, and E122Q spectra, although the 850- and 858-cm^{-1} bands are often not completely resolved. In E122Q, the broad ~853-cm^{-1} band has decreased in intensity relative to the 875-cm^{-1} band, and two overlapping lines are found at 847 and 858 cm^{-1}. The 847-cm^{-1} line is probably due to a downshifted C_{14}–H wag. The other observed HOOP vibrations of bathorhodopsin appear unchanged from those of the wild-type.

Raman spectra of the acidic forms of the E113Q and E113A pigments are shown in Figures 3 and 4. In the protonated Schiff base region, lines are observed at 1648 and 1645 cm^{-1} in E113Q and E113A, respectively, which downshift to 1629 and 1630 cm^{-1} in D_2O (Figures 3 and 4). The D_2O effect demonstrates that these lines are due to a protonated Schiff base linkage between the chromophore and the protein. The Raman spectra of E113Q and E113A are dominated by scattering from isorhodopsin. The lines at ~1150, 1205, and 1320 cm^{-1} which are characteristic for the 9-cis component (Palings et al., 1987) are more intense in the two Glu^{113} mutants than in the wild-type (Figure 4). The main C=C mode of isorhodopsin is downshifted to 1543 cm^{-1} in E113Q and 1546 cm^{-1} in E113A. The ethylenic frequency of bathorhodopsin is also lower in E113Q, but it is unshifted in E113A.

The mutation of Glu^{113} also affects vibrations in the HOOP region of bathorhodopsin. The ~888- and ~934-cm^{-1} modes in the E113Q and E113A spectra are assigned to the HOOP vibrations of bathorhodopsin because of their reduced intensity

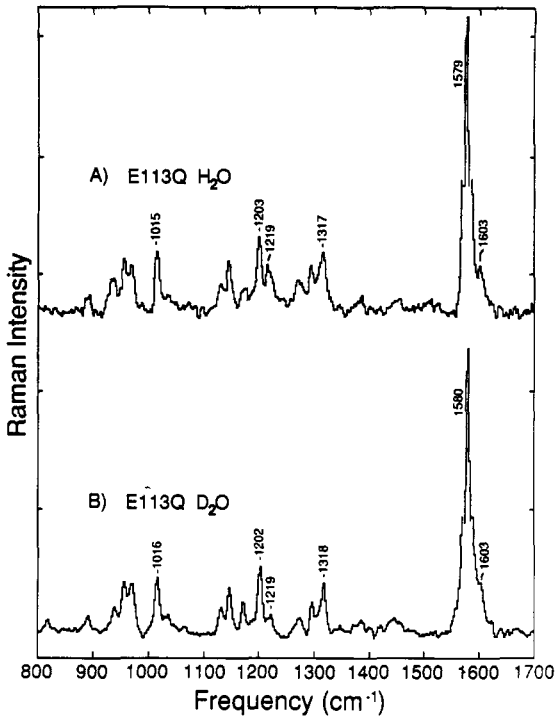

FIGURE 5: Raman microprobe spectra of the basic (pH 7.4) forms of E113Q in H_2O (A) and D_2O (B) at 77 K. The excitation wavelength was 413.1 nm.

in the pump–probe spectra (Figure 4). On the basis of frequency correspondence, the ~934-cm^{-1} band is assigned to the C_{11}–H wag and the 888-cm^{-1} mode to the C_{10}–H wag. The C_{12}–H and C_{14}–H HOOP modes which appear as a broad band at ~853 cm^{-1} in native bathorhodopsin have either lost intensity or shifted up underneath the 888-cm^{-1} band (see Discussion).

Raman spectra of the basic 380-nm E113Q pigment in H_2O and D_2O are presented in Figure 5. The fingerprint regions of these spectra qualitatively resemble those of Schiff base model compounds (Cookingham et al., 1978). In particular, the similarity of the 900–1400-cm^{-1} region of the spectra to those of 11-cis and 9-cis Schiff bases suggests that the 380-nm pigment sample consists of a mixture of these isomers under our irradiation conditions. The protonation state of retinal Schiff bases can be inferred from the frequency of the C_{12}–C_{13} stretching mode. The dominant effect of Schiff base protonation on the C–C stretches is to raise the frequency of the C_{14}–C_{15} mode which then pushes up the C_{12}–C_{13} mode from ~1225 to ~1240 cm^{-1} due to stronger interaction between the two coordinates (Mathies et al., 1987; Palings et al., 1987). The 1203- and 1219-cm^{-1} lines in the 380-nm pigment spectra can be assigned to the C_8–C_9 and C_{12}–C_{13} stretching modes, respectively, on the basis of fingerprint correlation diagrams by Palings et al. (1987). The 1219-cm^{-1} value of the C_{12}–C_{13} frequency is therefore consistent with the chromophore having an unprotonated Schiff base. In addition, lines assignable to the C=NH stretching vibration of a protonated species or to the C=O stretch of an aldehyde are not detected in the 1630–1660-cm^{-1} region, and no shifts are observed near 970, 1350, or 1650 cm^{-1} in D_2O that might indicate the presence of an exchangeable N–H group (Figure 5). The spectrum of the 380-nm-absorbing E113A pigment (not shown) is identical to that of E113Q.

Discussion

The resonance Raman microprobe system circumvents many of the problems associated with Raman spectroscopic studies

of mutant pigments and natural pigments that are difficult to isolate in large quantities. First, because the spectroscopy is performed in a microscope, the samples can be microscopic in size, and the collection of Raman scattered light from the irradiated area is maximized by the use of high numerical aperture objectives. Second, the CCD detector is a nearly ideal spectroscopic device because of its large photosensitive area and high quantum efficiency. Since the 1152 × 298 array of the CCD is twice the width of typical detector arrays, a single exposure provides a broad ~1400-cm^{-1} window in the visible region. Moreover, the high quantum efficiency assures very efficient light detection, and the low readout noise and dark current permit long integration times. Finally, sample degradation and photochemistry are controlled by cooling the sample to 77 K using the cold stage. These characteristics make it possible to obtain high signal-to-noise spectra of a pigment from as little as 5 μL of solution containing ~8 μg of protein. A wide variety of studies should be facilitated by the capabilities of this apparatus.

Rhodopsin Mutant Data. In this report, we present the first resonance Raman spectra of bovine rhodopsin mutants. These data provide new structural information about the role of residues Glu^{122}, Glu^{134}, and Glu^{113} in determining the spectral properties of rhodopsin. Glu^{134} has previously been located at the cytoplasmic border of the third transmembrane helix in a secondary structure model of rhodopsin (Franke et al., 1990; Sakmar et al., 1989). The Raman data from E134Q support this model. The similarity of the E134Q and COS cell rhodopsin Raman spectra shows that Glu^{134} is not located near the chromophore and suggests that it is not in the transmembrane part of the helix facing the protein interior. If Glu^{134} played an important function in maintaining the tertiary structure of the protein, its mutation would be expected to perturb the chromophore vibrations.

Substitution of Glu^{122} causes small perturbations of the bathorhodopsin HOOP lines and a general blue-shift of the λ_{max} of the chromophore in rhodopsin, bathorhodopsin, and isorhodopsin which is reflected in the upshifted C=C stretching frequencies. These changes do not appear to result from differences in the direct interaction between the Schiff base group and the protein because the frequencies of the C=NH stretching mode, and hence the Schiff base environments, in E122Q and the wild-type are the same. Perturbations near the Schiff base would be manifested as a shift of the C=NH band (Baasov et al., 1987; Deng & Callender, 1987; Kakitani et al., 1983; Rodman Gilson et al., 1988). The C_{11}–H and C_{12}–H wag frequencies and intensities are also unchanged in the bathorhodopsin of E122Q. However, the downshift of presumably the C_{14}–H wag suggests that the protein environment around C_{14} is slightly different (Eyring et al., 1980, 1982). These changes are most likely due to an indirect steric effect because absorption blue-shifts of similar magnitude are also observed in E122A and E122D mutants (Nakayama & Khorana, 1991; Sakmar et al., 1989).

The changes in the resonance Raman spectra of E113Q and E113A are consistent with those expected from the modification of the primary counterion environment of the PSB group. The C=NH frequencies in E113Q and E113A are shifted down by ~10 cm^{-1} from the value in the wild-type spectrum, and their shifts in D_2O (~17 cm^{-1}) are significantly smaller than those measured in native bathorhodopsin and isorhodopsin (~25 cm^{-1}), and in model PSB compounds in methanol (Deng & Callender, 1987; Palings et al., 1987). The reduced frequency and D_2O shift of the C=NH stretching vibration in the acidic form of these mutants indicate that the electrostatic interaction between the halide that replaces Glu^{113} in E113Q and E113A (Nathans, 1990b; Sakmar et al., 1991) and the Schiff base group is reduced. This conclusion is supported by model compound studies (Baasov et al., 1987), by calculations (Deng & Callender, 1987; Rodman Gilson et al., 1988), and by analogy with the earlier interpretation of the spectra of bacteriorhodopsin, halorhodopsin, and sensory rhodopsin (Fodor et al., 1989), which correlated a lower C=NH stretching frequency and smaller D_2O shift with a weaker hydrogen-bonding (electrostatic) interaction between the Schiff base group and its counterion. Consistent with this interpretation, the pK_a of the Schiff base is lowered to ~6 in the Glu^{113} mutants from >9 in the native pigment. The 380-nm forms of E113Q and E113A are thought to contain a deprotonated Schiff base chromophore (Sakmar et al., 1989; Zhukovsky & Oprian, 1989). The Raman spectra of the 380-nm pigments support this proposal. The ~1220-cm^{-1} frequency of the fingerprint line assigned to the C_{12}–C_{13} mode and the absence of bands between 1640 and 1660 cm^{-1} are characteristics of unprotonated retinal Schiff bases. The strong perturbation on the vibrational and thermodynamic properties of the retinal PSB group when a neutral residue occupies the 113-position supports the idea that Glu^{113} is the primary counterion. In bacteriorhodopsin, the loss of the negative charge supplied by Asp^{85} causes a red-shift of the absorption, an anion dependence of the absorption band, and a lowering of the Schiff base pK_a (Marti et al., 1991) that are very similar to the behavior observed in the Glu^{113} mutants of rhodopsin.

Interpretation of Bathorhodopsin Mutant Data. The intense 853-, 875-, and 921-cm^{-1} HOOP lines of bathorhodopsin arise from unique structural perturbation of its nominally 11-*trans*-retinal chromophore. Their intensities arise from torsional distortions of the polyene. The anomalous decoupling of the 921-cm^{-1} C_{11}–H wag from the C_{12}–H wag results from a protein perturbation near C_{12} which lowers the C_{12}–H wag frequency (Eyring et al., 1982; Palings et al., 1989; Smith et al., 1991). The Raman spectra of E113Q and E113A show that these vibrations are significantly modified by the substitution at 113. The C_{11}–H wag shifts up by ~10 cm^{-1} to ~934 cm^{-1}. The C_{10}–H wag also shifts up ~10 cm^{-1} to 887 cm^{-1}, and it appears that the C_{12}–H and C_{14}–H wags shift up underneath the C_{10}–H wag. A consistent explanation for these observations is that the C_{12}–H wag vibration is less perturbed in the Glu^{113} mutants and moves up in frequency. This would allow it to couple more effectively with the C_{11}–H wag, pushing the C_{11}–H wag up in frequency as well. One would expect that the 934-cm^{-1} mode will pick up C_{12}–H wag character, becoming more like a coupled $C_{11}H{=}C_{12}H$ A_u mode. However, its 934-cm^{-1} frequency is still well below the expected 960–970-cm^{-1} range, indicating that the C_{11}–H and C_{12}–H coupling is still unusually low.

The resonance Raman spectra of the Glu^{113} mutants presented here are surprisingly similar to the spectra of octopus (Deng et al., 1991) and squid (Sulkes et al., 1978) rhodopsins which also lack a carboxylate group at the 113-position (Hall et al., 1991; Ovchinnikov et al., 1988). A Tyr residue occupies the location in the octopus and squid primary structure analogous to that of Glu^{113} in bovine rhodopsin. The octopus and squid bathorhodopsin spectra have strong bands at ~887 and 940 cm^{-1} which are very similar to those observed in E113Q and E113A. The normal mode character of these lines in octopus bathorhodopsin has been investigated using deuterium-labeled chromophores (Deng et al., 1991). The 887-cm^{-1} band consists of the degenerate C_{10}–H and C_{14}–H wags with most of the intensity coming from the C_{10}–H wag. The

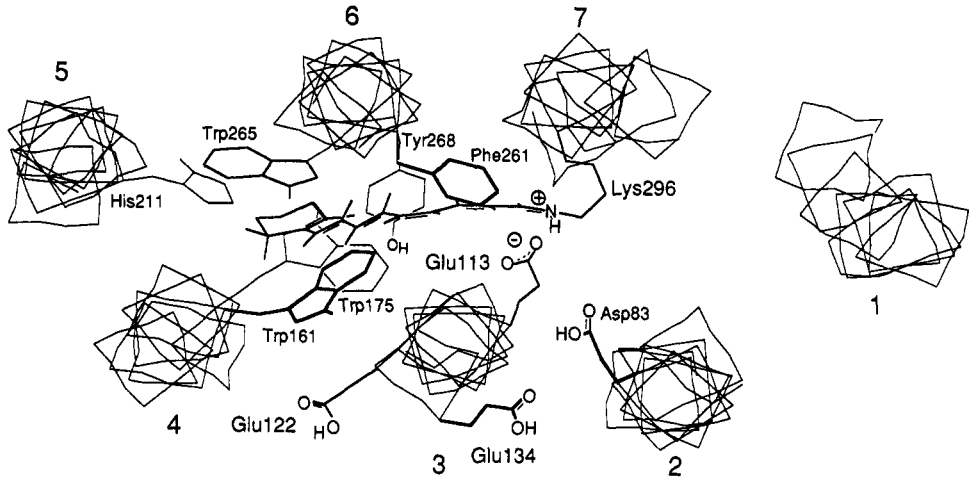

FIGURE 6: Molecular graphics model of bovine rhodopsin. The view is perpendicular to the plane of the disk membrane from above the cytoplasmic surface.

940-cm^{-1} line is due to the $C_{11}H$–wag that is coupled to the C_{12}–H wag. The C_{12}–H wag is estimated to lie near 880 cm^{-1}, about 20 cm^{-1} higher than the frequency in bovine bathorhodopsin (Palings et al., 1989). On the basis of the similarities of the resonance Raman spectra and of the changes in the primary structure, it is reasonable to assume that these assignments for octopus rhodopsin should also apply to the Glu^{113} mutants and that the binding site structure for octopus rhodopsin is similar to that of the Glu^{113} mutants.

These vibrational assignments provide insight into the binding site structure of bovine bathorhodopsin. The absence of a Glu counterion in the visual pigments is correlated with a weaker protein perturbation near the C_{12}-position of the bathorhodopsin chromophore, and this mutation also reduces the electrostatic stabilization of the PSB group. *These results indicate that the negatively charged Glu^{113} electrostatically stabilizes the positively charged Schiff base group and also perturbs the C_{12}–H wagging mode of the chromophore in bathorhodopsin.* These interactions are presumably facilitated by the two oxygen atoms of the carboxylate group which can be oriented to interact preferentially with both the C_{12}-position and the Schiff base group. When the carboxylate group is removed, the halide which replaces it cannot span this distance, and the chromophore interaction at the Schiff base and C_{12} positions is reduced. These results and interpretation support the model of the chromophore binding site proposed by Birge and co-workers (Birge et al., 1988) in which a carboxylate counterion is positioned perpendicular to the chromophore plane such that one of the oxygen atoms is located close to the nitrogen atom and the other is in the vicinity of C_{13} and C_{15}.

Structural Model for Rhodopsin. A model for the binding site of rhodopsin that is consistent with the available data is presented in Figure 6. The transmembrane helices have been arranged clockwise in analogy to the bacteriorhodopsin structure (Henderson et al., 1990). The surfaces of all helices except that of helix 3 have been oriented according to the model of Rees et al. (1989). Helix 3 was rotated to position Glu^{113} near the PSB moiety while maintaining the general relative orientation of the carboxylate and the PSB groups proposed by Birge et al. (1988). One of the oxygen atoms of Glu^{113} is positioned ~3 Å from the Schiff base nitrogen, and the other is ~4 Å from C_{13}. The exact hydrogen-bonding of the Schiff base group is unknown and may involve water molecules which are thought to lie in the retinal binding site (Rafferty & Shichi, 1981; Birge, 1990). The placement of Glu^{113} determines the vertical location of helix 3 in the membrane and also constrains Glu^{122} to be located at the interface with helix 4. This location is consistent with the lack of change seen in the Schiff base environment in the Raman spectrum of E122Q. The model suggests that the structural perturbation in E122Q is probably localized near the ionone ring and could result from the disruption of normal steric interaction between helices 3 and 4. The approximate 20-nm blue-shifts of the λ_{max} values of rhodopsin, bathorhodopsin, and isorhodopsin in E122Q may be explained by a different electrostatic environment around the ring. In addition, this location precludes Glu^{122} from serving as an alternate counterion. Finally, Glu^{134} is located ~10 Å from the center of the chromophore at the cytoplasmic border of helix 3.

Conclusions

Our experiments on rhodopsin mutants demonstrate the feasibility and the utility of performing resonance Raman microprobe spectroscopy on minute amounts of visual pigments in order to obtain specific information on chromophore structure and protein–chromophore interactions. Further studies of rhodopsin mutants should allow us to develop and refine models for the structure of the retinal binding pocket. In particular, it will be interesting to use isotopically substituted chromophores to assign the specific HOOP vibrations in rhodopsin mutants as has been done previously for native bovine rhodopsin (Eyring et al., 1982; Palings et al., 1989) and octopus rhodopsin (Deng et al., 1991). Finally, it should now be possible to obtain resonance Raman spectra of expressed cone pigments to investigate the mechanism of spectral tuning in visual pigments.

Registry No. Glu, 56-86-0.

References

Abraham, J. L., & Etz, E. S. (1979) *Science 206*, 716–718.
Baasov, T., Friedman, N., & Sheves, M. (1987) *Biochemistry 26*, 3210–3217.
Barry, B., & Mathies, R. (1982) *J. Cell Biol. 94*, 479–482.
Barry, B., & Mathies, R. A. (1987) *Biochemistry 26*, 59–64.
Barry, B., Mathies, R. A., Pardoen, J. A., & Lugtenburg, J. (1987) *Biophys. J. 52*, 603–610.
Birge, R. R. (1990) *Biochim. Biophys. Acta 1016*, 293–327.
Birge, R. R., Murray, L. P., Pierce, B. M., Akita, H., Balogh-Nair, V., Findsen, L. A., & Nakanishi, K. (1985) *Proc. Natl. Acad. Sci. U.S.A. 82*, 4117–4121.
Birge, R. R., Einterz, C. M., Knapp, H. M., & Murray, L. P. (1988) *Biophys. J. 53*, 367–385.

Blatz, P. E., Mohler, J. H., & Navangul, H. V. (1972) *Biochemistry 11*, 848–855.
Cookingham, R. E., Lewis, A., & Lemley, A. T. (1978) *Biochemistry 17*, 4699–4711.
Deng, H., & Callender, R. H. (1987) *Biochemistry 26*, 7418–7426.
Deng, H., Manor, D., Weng, G., Rath, P., Koutalos, Y., Ebrey, T., Gebhard, R., Lugtenburg, J., Tsuda, M., & Callender, R. H. (1991) *Biochemistry 30*, 4495–4502.
Doukas, A. G., Aton, B., Callender, R. H., & Ebrey, T. G. (1978) *Biochemistry 17*, 2430–2435.
Eyring, G., & Mathies, R. (1979) *Proc. Natl. Acad. Sci. U.S.A. 76*, 33–37.
Eyring, G., Curry, B., Mathies, R., Fransen, R., Palings, I., & Lugtenburg, J. (1980) *Biochemistry 19*, 2410–2418.
Eyring, G., Curry, B., Broek, A., Lugtenberg, J., & Mathies, R. (1982) *Biochemistry 21*, 384–393.
Ferretti, L., Karnik, S. S., Khorana, H. G., Nassal, M., & Oprian, D. D. (1986) *Proc. Natl. Acad. Sci. U.S.A. 83*, 599–603.
Fodor, S. P. A., Gebhard, R., Lugtenburg, J., Bogomolni, R. A., & Mathies, R. A. (1989) *J. Biol. Chem. 264*, 18280–18283.
Franke, R. R., Sakmar, T. P., Oprian, D. D., & Khorana, H. G. (1988) *J. Biol. Chem. 263*, 2119–2122.
Franke, R. R., König, B., Sakmar, T. P., Khorana, H. G., & Hofmann, K. P. (1990) *Science 250*, 123–125.
Hall, M. D., Hoon, M. A., Ryba, N. J. P., Pottinger, J. D. D., Keen, J. N., Saibil, H. R., & Findlay, J. B. C. (1991) *Biochem. J. 274*, 35–40.
Henderson, R., Baldwin, J. M., Ceska, T. A., Zemlin, F., Beckmann, E., & Downing, K. H. (1990) *J. Mol. Biol. 213*, 899–929.
Honig, B., Greenberg, A. D., Dinur, U., & Ebrey, T. G. (1976) *Biochemistry 15*, 4593–4599.
Honig, B., Dinur, U., Nakanishi, K., Balogh-Nair, V., Gawinowicz, M. A., Arnaboldi, M., & Motto, M. G. (1979) *J. Am. Chem. Soc. 101*, 7084–7086.
Kakitani, H., Kakitani, T., Rodman, H., Honig, B., & Callender, R. (1983) *J. Phys. Chem. 87*, 3620–3628.
Koutalos, Y., Ebrey, T. G., Tsuda, M., Odashima, K., Lien, T., Park, M. H., Shimizu, N., Derguini, F., Nakanishi, K., Gilson, H. R., & Honig, B. (1989) *Biochemistry 28*, 2732–2739.
Loppnow, G. R., & Mathies, R. A. (1989) *Rev. Sci. Instrum. 60*, 2628–2630.
Loppnow, G. R., Barry, B. A., & Mathies, R. A. (1989) *Proc. Natl. Acad. Sci. U.S.A. 86*, 1515–1518.
Marti, T., Rösselet, S. J., Otto, H., Heyn, M. P., & Khorana, H. G. (1991) *J. Biol. Chem. 266*, 18674–18683.
Mathies, R., & Yu, N.-T. (1978) *J. Raman Spectrosc. 7*, 349–352.
Mathies, R. A., Smith, S. O., & Palings, I. (1987) *Biological Applications of Raman Spectroscopy* (Spiro, T. G., Ed.) Vol. 2, pp 59–108, John Wiley and Sons, New York.
Nakayama, T. A., & Khorana, H. G. (1991) *J. Biol. Chem. 266*, 4269–4275.
Nathans, J. (1990a) *Biochemistry 29*, 937–942.
Nathans, J. (1990b) *Biochemistry 29*, 9746–9752.
Oprian, D. D., Molday, R. S., Kaufman, R. J., & Khorana, H. G. (1987) *Proc. Natl. Acad. Sci. U.S.A. 84*, 8874–8878.
Oseroff, A. R., & Callender, R. H. (1974) *Biochemistry 13*, 4243–4248.
Ottolenghi, M., & Sheves, M. (1989) *J. Membr. Biol. 112*, 193–212.
Ovchinnikov, Yu. A., Abdulaev, N. G., Zolotarev, A. S., Artamonov, I. D., Bespalov, I. A., Dergachev, A. E., & Tsuda, M. (1988) *FEBS Lett. 232*, 69–72.
Palings, I., Pardoen, J. A., van den Berg, E., Winkel, C., Lugtenburg, J., & Mathies, R. A. (1987) *Biochemistry 26*, 2544–2556.
Palings, I., van den Berg, E. M. M., Lugtenburg, J., & Mathies, R. A. (1989) *Biochemistry 28*, 1498–1507.
Puppels, G. J., de Mul, F. F. M., Otto, C., Greve, J., Robert-Nicoud, M., Arndt-Jovin, D. J., & Jovin, T. M. (1990) *Nature 347*, 301–303.
Rafferty, C. N., & Shichi, H. (1981) *Photochem. Photobiol. 33*, 229–234.
Rees, D. C., DeAntonio, L., & Eisenberg, D. (1989) *Science 245*, 510–513.
Rimai, L., Heyde, M. E., & Gill, D. (1973) *J. Am. Chem. Soc. 95*, 4493–4501.
Rodman Gilson, H. S., Honig, B. H., Croteau, A., Zarrilli, G., & Nakanishi, K. (1988) *Biophys. J. 53*, 261–269.
Rosasco, G. J. (1980) *Adv. Infrared Raman Spectrosc. 7*, 223–282.
Sakmar, T. P., Franke, R. R., & Khorana, H. G. (1989) *Proc. Natl. Acad. Sci. U.S.A. 86*, 8309–8313.
Sakmar, T. P., Franke, R. R., & Khorana, H. G. (1991) *Proc. Natl. Acad. Sci. U.S.A. 88*, 3079–3083.
Smith, S. O., Palings, I., Miley, M. E., Courtin, J., de Groot, H., Lugtenburg, J., Mathies, R. A., & Griffin, R. G. (1990) *Biochemistry 29*, 8158–8164.
Smith, S. O., Courtin, J., de Groot, H., Gebhard, R., & Lugtenburg, J. (1991) *Biochemistry 30*, 7409–7415.
Smulevich, G., Wang, Y., Edwards, S. L., Poulos, T. L., English, A. M., & Spiro, T. G. (1990) *Biochemistry 29*, 2586–2592.
Sulkes, M., Lewis, A., & Marcus, M. A. (1978) *Biochemistry 17*, 4712–4722.
Yoshizawa, T., & Wald, G. (1963) *Nature (London) 197*, 1279–1286.
Zhukovsky, E. A., & Oprian, D. D. (1989) *Science 246*, 928–930.